Flexible Multielectrode Arrays With 2-D and 3-D Contacts for *In Vivo* Electromyography Recording

Muneeb Zia [Member, IEEE],

Department of Electrical and Computer Engineering, Georgia Institute of Technology, Atlanta, GA 30332 USA

Bryce Chung,

Department of Biology, Emory University, Atlanta, GA 30322 USA

Samuel Sober,

Department of Biology, Emory University, Atlanta, GA 30322 USA

Muhannad S. Bakir [Senior Member, IEEE]

Department of Electrical and Computer Engineering, Georgia Institute of Technology, Atlanta, GA 30332 USA

Abstract

We present a system for recording *in vivo* electromyographic (EMG) signals from songbirds using hybrid polyimide–polydimethylsiloxane (PDMS) flexible multielectrode arrays (MEAs). 2-D electrodes with a diameter of 200, 125, and 50 μm and a center-to-center pitch of 300, 200, and 100 μm, respectively, were fabricated. 3-D MEAs were fabricated using a photoresist reflow process to obtain hemispherical domes utilized to form the 3-D electrodes. Biocompatibility and flexibility of the arrays were ensured by using polyimide and PDMS as the materials of choice for the arrays. EMG activity was recorded from the expiratory muscle group of anesthetized songbirds using the fabricated 2-D and 3-D arrays. Air pressure data were also recorded simultaneously from the air sac of the songbird. Together, EMG recordings and air pressure measurements can be used to characterize how the nervous system controls breathing and other motor behaviors. Such technologies can in turn provide unique insights into motor control in a range of species, including humans. An improvement of over 7× in the signal-to-noise ratio (SNR) is observed with the utilization of 3-D MEAs in comparison to 2-D MEAs.

Keywords

Electromyography; flexible multielectrode arrays (MEAs); polydimethylsiloxane (PDMS); polyimide; songbird

---

I. Introduction

Evolution of data analysis methods in neuroscience in the recent past has increased our collective understanding of how a nervous system controls complex behaviors, including,

Corresponding author: Muneeb Zia, muneeb.zia@gatech.edu.

but not limited to, vocal learning and song production in songbirds [1]–[4]. This research focuses largely on the central nervous system, exploiting new technologies that can record large numbers of individual neurons (brain cells) for extended periods of time in order to quantify their relation to behavior [5]–[7]. Despite recent evidence pointing to the importance of precise timing in the activity of motor units (collection of muscle fibers innervated by a single motor neuron) for controlling behavior [3], [4], techniques for recording electromyographic (EMG) signals from muscles lag far behind those developed for neural recordings in the central nervous system. Specifically, most EMG data sets are collected by inserting fine-wire electrodes into the muscles. This method has several drawbacks. First, the penetrating wire electrodes damage the muscles into which they are inserted and cannot be used to record the very small muscles that control skilled behavior. Second, wire electrodes typically cannot isolate electrical signals from individual motor units, instead yield signals that represent the combined activity of many units, preventing analysis of single-unit activity (a standard approach for studying the function of neurons in the brain). New approaches are therefore needed to record stable, single-unit, EMG activity.

Information-theoretic analyses provide a quantitative framework to understand how time series of electrical events (action potentials or "spikes") in biological tissues represent information and control behavior [3], [4], [8]–[10]. For example, in a recent study, EMG signals from expiratory muscles in songbirds Fig. 1(a) were recorded using multielectrode arrays (MEAs) [3]. Spike-sorting routines [11], [12] were used to identify spikes [tick marks in Fig. 1(b)] from individual motor units, which arise when a motor neuron activates a set of muscle fibers and causes them to contract [13]. Information-theoretic techniques were used to correlate the timing of spikes with fluctuations in air pressure within the respiratory system [Fig. 1(b)]. Although this article provided evidence for the importance of precise spike timing in individual motor units for controlling the respiratory behavior [3], the difficulty in robustly recording multiple units simultaneously and over long periods limits our understanding of how the nervous system controls complex behaviors.

A key challenge in characterizing single motor unit activity is obtaining stable, reliable EMG recordings for long enough duration that can yield data sets that are large enough to perform advanced computational analyses (including, but not limited to, information-theoretic methods) [9], [14]. While advances in spike-sorting algorithms [12], [15], [16] have helped to better discriminate multiple units recorded on the same channel, the ability to record single units on an MEA channel remains essential to such research efforts.

Current technologies employ flexible polymers, such as polyimide [3], [17], [18], polydimethylsiloxane (PDMS) [19], [20], and parylene-C [21], [22], as the substrate for the MEA and use metals like gold for contact sites. MEA fabrication is also beginning to combine materials in order to optimize the processing parameters and mechanical properties of different polymers [23], [24] as well as to utilize modified silicone polymers [25]. The advantage of using these materials includes their compatibility with muscles and other tissues as well as their biocompatibility. However, each of these materials have their own processing challenges: PDMS suffers from poor metal adhesion [26]–[28] and polyimide typically requires a metal etch mask [29], [30] or, in the case of photo-definable polyimide, is significantly more expensive. In this article, we present a hybrid polyimide-PDMS 2-D

and 3-D MEA fabrication process leveraging the benefits of each of the materials while mitigating their shortcomings. Using a 2-D MEA with the hybrid polyimide–PDMS substrate resulted in EMG recordings that were better than those obtained using a pair of fine-wire electrodes inserted into muscles. Owing to the high signal-to-noise ratio (SNR) of the 3-D MEAs, small units can also be detected, which otherwise would be masked by noise.

II. Fabrication of 2-D and 3-D MEAs

The fabrication of 2-D and 3-D MEAs is summarized in Fig. 2. A base layer of polyimide is first spin-coated and cured; this serves as the substrate for subsequent fabrication steps. The traces for the MEAs are then fabricated followed by spin-coating of PDMS to serve as the top insulation layer for the 2-D MEAs. The electrode and the connector sites on the MEAs are then exposed by etching the PDMS from those areas.

To obtain the 3-D MEAs, a photoresist reflow process is utilized to form the hemispherical domes [shown in step (e) in Fig. 2] after the lift-off process step [step (d) in Fig. 2]. The profile of the domes obtained from this process is shown in Fig. 3. The double-reflow process described in [31] can also be utilized to fabricate domes of varying heights, which will allow multiheight 3-D electrode formation in the same process. After the dome formation, the 3-D electrode sites are electroplated followed by the removal of seed layer and sacrificial photoresist dome layer. The electroplated surface is then passivated using electroless gold. Similar to 2-D MEAs, PDMS is used as the top insulation and a subsequent etch process is then utilized to expose the electrode site. Further details of formation of 3-D MEAs can be found in [32]. Optical images of the fabricated 2-D and 3-D electrodes are shown in Figs. 4 and 5 respectively.

III. MEA Characterization and EMG Measurements

A. Electrical Characterization of Fabricated 2-D MEAs

Four-point resistance measurements for the trace and electrodes on the fabricated devices were performed, as shown in Fig. 6. The average resistance of the traces and the electrode impedance for the 200-, 125-, and 50-μm diameter electrodes was measured to be 234 Ω. The electrode size did not impact the dc resistance significantly as the resistance was primarily determined by the metal trace. To characterize biologically relevant electrical properties, the impedance at 1000 Hz was measured with an Intan RHD2000 Eval board (Intan Technologies). The MEA devices were submerged in a grounded bath of saline (10% saline solution, TEKNOVA) and connected via a zero-insertion-force (ZIF)-clip/Omnetics adapter to an Intan RHD 2132 amplifier board [Intan Technologies; Fig. 6(b)]. The average impedances for the 200-, 125-, and 50-μm diameter 2-D electrodes were measured to be 77, 107, and 556 kΩ, respectively, while the average impedance of the 3-D electrodes was measured to be 67 kΩ.

B. EMG Measurements

A data collection flowchart from the songbird experiment is summarized in Fig. 7. The air pressure inside the air sac and the EMG activity from the expiratory muscle of the songbird are simultaneously recorded. An Intan amplifier (RHD 2216) coupled with an evaluation

board (RHD 2000) is used to amplify and digitize the recorded EMG signal. The evaluation board also records air pressure data for analysis. Spike sorting is used to identify motor units, which can then be used for mutual information assessment.

EMG activity was recorded from the expiratory muscles of anesthetized songbirds using the flexible MEA devices described above or a pair of fine-wire electrodes made from 25-μm diameter stainless steel wire. All procedures performed had been approved by the Emory University Institutional Animal Care and Use Committee. EMG recordings for the polyimide-PDMS devices were collected using 16 electrode sites that were 200, 125, and 50 μm in diameter and were placed in a 2-D array with equal spacing. An Intan RHD2216 bipolar amplifier was used to subtract and amplify voltage signals from pairs of EMG electrode contacts, yielding eight bipolar recordings. Based on the physiological properties (relative amplitude, type of burst, etc.), example EMG units on electrode pairs were selected.

The EMG units shown here (Fig. 8) fired rhythmically throughout the expiration phase of each breathing cycle. These EMG units were also the smallest units identified within each recording. A qualitative comparison of different electrode diameters [Fig. 8(a)–(c)] does not show significant differences in signal fidelity. To illustrate the extent to which the MEAs represent a significant improvement over standard, fine-wire EMG techniques, Fig. 8(d) shows a fine-wire recording from the expiratory muscle. As is typical for wire EMG recordings, the recorded signal consists of many overlapping spike waveforms [in comparison with the isolated recordings of single units shown in Fig. 8(a)–(c)].

C. SNR Comparison for Fabricated 2-D and 3-D MEAs

The fabricated 2-D and 3-D MEAs at 300-μm pitch were used to measure EMG for SNR comparison. The EMG recordings were carried out for 30 min each and alternated between the 2-D and 3-D MEAs. The muscle surface was kept moist by putting a drop of saline in-between recordings. Care was taken to make sure that the electrodes are placed over the same location of the expiratory muscle of the bird. The SNR was measured within the same recordings and was calculated as an average of multiple samples from different time points within each 1-min recording. Due to the rhythmicity of expiratory muscle activity, EMG electrodes did not detect activity between periods of exhalation. The root-mean-square (rms) values of the amplitude of the signal and noise during a period of activity and no-activity, respectively, were used to determine the SNR. Fig. 9(a) shows the SNR for the 2-D and 3-D MEAs for the four experiments that were performed. Fig. 9(b) depicts a sample EMG signal with highlighted signal and noise regions—rms values of the amplitude were calculated for signal and noise using the green and red shaded regions of the EMG signal, respectively, to obtain the SNR values. The error bars in Fig. 9(a) denote the standard error of mean. The lower SNR of the 2-D electrodes can be attributed to the higher electrode impedance due to the lower surface area [33]–[35]; the 3-D electrodes, on the other hand, provide a larger surface area with the same footprint as that of 2-D electrodes which in turn results in a lower electrode impedance and a higher SNR. Furthermore, since the 2-D electrodes are inset below the top insulation layer, they are also more susceptible to protein buildup on the electrode surface during the course of an *in vivo* measurement, which also translates into a

higher electrode impedance. The 3-D MEAs provide higher SNR throughout the course of the experiment with up to 7× higher SNR for the larger unit.

IV. Conclusion

In vivo EMG recordings from breathing muscles of a songbird utilizing hybrid polyimide-PDMS flexible MEAs with 2-D and 3-D electrodes are presented. The lithography-based process enables ease of fabrication and scalability for the MEAs. The fabrication process for obtaining the 3-D contacts allows for easy height modulation of the electrodes by modifying the photoresist thickness. EMG activity from the expiratory muscle of the bird as well as the air pressure data are simultaneously recorded using the Intan amplifier and evaluation board. The fabricated 3-D MEA presented here further improves the SNR of the EMG recordings by providing better muscle contact and a higher surface area; the 3-D MEAs can sustain a higher SNR over an extended period, as compared to the 2-D MEAs. This enables detection of smaller amplitude units, which are otherwise masked by noise, and hence provide a reliable and holistic measurement; this in turn would enable a better and more complete understanding of the precise mechanism by which the nervous system controls behavior.

Acknowledgments

References

[1]. Mackavicius EL and Fee MS, "Building a state space for song learning," Curr. Opin. Neurobiol, vol. 49, pp. 59–68, 4 2018. [PubMed: 29268193]

[2]. Srivastava KH, Elemans CPH, and Sober SJ, "Multifunctional and context-dependent control of vocal acoustics by individual muscles," J. Neurosci, vol. 35, no. 42, pp. 14183–14194, 10 2015. [PubMed: 26490859]

[3]. Srivastava KH, "Motor control by precisely timed spike patterns," Proc. Natl. Acad. Sci. USA, vol. 114, no. 5, pp. 1171–1176, 1 2017. [PubMed: 28100491]

[4]. Tang C, Chehayeb D, Srivastava K, Nemenman I, and Sober SJ, "Millisecond-scale motor encoding in a cortical vocal area," PLoS Biol, vol. 12, no. 12, 12 2014, Art. no. e1002018. [PubMed: 25490022]

[5]. Guitchounts G, Markowitz JE, Liberti WA, and Gardner TJ, "A carbon-fiber electrode array for long-term neural recording," J. Neural Eng, vol. 10, no. 4, 7 2017, Art. no 046016.

[6]. Lin L, Osan R, Shoham S, Jin W, Zuo W, and Tsien JZ, "Identification of network-level coding units for real-time representation of episodic experiences in the hippocampus," Proc. Natl. Acad. Sci. USA, vol. 102, no. 17, pp. 6125–6130, 4 2005. [PubMed: 15833817]

[7]. Churchland MM, "Neural population dynamics during reaching," Nature, vol. 487, no. 7405, pp. 51–56, 7 2012. [PubMed: 22722855]

[8]. Nemenman I, Shafee F, and Bialek W, "Entropy and inference, revisited," in Advances in Neural Information Processing Systems, vol. 14, Dietterich TG, Becker S and Ghahramani Z, Eds. Cambridge, MA, USA: MIT Press, 2002.

[9]. Kraskov A, Stogbauer H, and Grassberger P, "Estimating mutual information," Phys. Rev. E, Stat. Phys. Plasmas Fluids Relat. Interdiscip. Top. Stat. Nonlin. Soft Matter. Phys, vol. 69, no. 6, 6 2004, Art. no. 66138.

[10]. Nemenman I, Lewen GD, Bialek W, and de Ruyter van Steveninck RR, "Neural coding of natural stimuli: Information a sub-millisecond resolution," PLoSComput. Biol, vol. 4, no. 3, 3 2008, Art. no. e1000025.

[11]. Sober SJ, Wohlgemuth MJ, and Brainard MS, "Central contributions to acoustic variation in birdsong," J. Neurosci, vol. 28, no. 41, pp. 10370–10379, 10 2008. [PubMed: 18842896]

[12]. Heitler WJ, "DataView: A tutorial tool for data analysis. Template-based spike sorting and frequency analysis," J. Undergrad. Neurosci. Educ, vol. 6, no. 1, pp. A1–A7, 10 2007. [PubMed: 23493818]

[13]. Siegelbaum SA and Hudspeth AJ, Prinicples of Neural Science, vol. 4, Kandel ER, Schwartz JH, and Jessell TM, Eds. New York, NY, USA: McGraw-Hill, 2000, pp. 768–789.

[14]. Nemenman I, Bialek W, and De Ruyter van Steveninck R, "Entropy and information in neural spike trains: Progress on the sampling problem," Phys. Rev. E, Stat. Phys. Plasmas Fluids Relat. Interdiscip. Top, vol. 69, no. 5, 5 2004, Art. no. 56111.

[15]. Kadir SN, Goodman DFM, and Harris KD, "High-dimensional cluster analysis with the masked EM algorithm," Neural Comput, vol. 26, no. 11, pp. 2379–2394, 11 2014. [PubMed: 25149694]

[16]. Rossant C, "Spike sorting for large, dense electrode arrays," Nature Neurosci, vol. 19, no. 4, pp. 634–641, 3 2016. [PubMed: 26974951]

[17]. Kim O et al., "Novel neural interface electrode array for the peripheral nerve," in Proc. Int. Conf. Rehabil. Robot. (ICORR), 7 2017, pp. 1067–1072.

[18]. Lin K, Wang X, Zhang X, Wang B, Huang J, and Huang F, "An FPC based flexible dry electrode with stacked double-micro-domes array for wearable biopotential recording system," Microsyst. Technol, vol. 23, no. 5, pp. 1443–1451, 5 2017.

[19]. Guvanasen GS, "A stretchable microneedle electrode array for stimulating and measuring intramuscular electromyograhpic activity," IIEEE Trans. Neural Syst. Rehabil. Eng, vol. 25, no. 9, pp. 1440–1452, 9 2017.

[20]. Kim JM, Im C, and Lee WR, "Plateau-shaped flexible polymer microelectrode array for neural recording," Polymers, vol. 9, no. 12, p. 690, 12 2017.

[21]. Metallo C, White RD, and Trimmer BA, "Flexible parylene-based microelectrode arrays for high resolution EMG recordings in freely moving small animals," J. Neurosci. Methods, vol. 195, no. 2, pp. 176–184, 2 2011. [PubMed: 21167202]

[22]. Nandra MS, Lavrov IA, Edgerton VR, and Tai Y-C, "A parylene-based microelectrode array implant for spinal cord stimulation in rats," in Proc. IEEE 24th Int. Conf. Micro Electro Mech. Syst., Jan. 2011, pp. 1007–1010.

[23]. Byun D, Cho SJ, Lee BH, Min J, Lee JH, and Kim S, "Recording nerve signals in canine sciatic nerves with a flexible penetrating microelectrode array," J. Neural Eng, vol. 14, no. 4, 6 2017, Art. no. 46023.

[24]. Lee WR, Im C, Koh CS, Kim JM, Sjhin HC, and Seo JM, "A convex-shaped, PDMS-parylene hybrid multichannel ECoGelectrode array," in Proc. 39th Annu. Int. Conf. IEEE Eng. Med. Biol. Soc. (EMBC), Jul. 2017, pp. 1093–1096.

[25]. Al-Othman A, Alatoom A, Farooq A, Al-Sayah M, and Al-Nashash H, "Novel flexible implantable electrodes based on conductive polymers and titanium dioxide," in Proc. IEEE 4th Middle East Conf. Biomed. Eng. (MECBME), Mar. 2018, pp. 30–33.

[26]. Guo L and Deweerth SP, "An effective lift-off method for patterning high-density gold interconnects on an elastomeric substrate," Small, vol. 6, no. 24, pp. 2847–2852, 12 2010. [PubMed: 21104803]

[27]. Lee M-T, Lee D, Sherry A, and Grigoropoulos CP, "Rapid selective metal patterning on polydimethylsiloxane (PDMS) fabricated by capillarity-assisted laser direct write," J. Micromech. Microeng, vol. 21, no. 9, 9 2011, Art. no. 95018.

[28]. Li L et al., "Nanofabrication on unconventional substrates using transferred hard masks," Sci. Rep, vol. 5, 1 2015, Art. no. 7802. [PubMed: 25588550]

[29]. Metz S, Oppliger F, Holzer R, Buisson B, Bertrand D, and Renaud P, "Fabrication and test of implantable thin-film electrodes for stimulation and recording of biological signals," in Proc. 1st Annu. Int. IEEE-EMBS Special Topic Conf. Microtechnol. Med. Biol., Nov. 2002, pp. 619–623.

[30]. Mimoun B, Pham HTM, Henneken V, and Dekker R, "Residue-free plasma etching of polyimide coatings for small pitch vias with improved step coverage," J. Vacuum Sci. Technol. B, Nanotechnol. Microelectron., Mater., Process., Meas., Phenom, vol. 31, no. 2, 3 2013, Art. no. 21201.

[31]. Zhang C, Yang HS, and Bakir MS, "A double-lithography and double-reflow process and application to multi-pitch multi-height mechanical flexible interconnects," J. Micromech. Microeng, vol. 27, no. 2, 2 2017, Art. no. 25014.

[32]. Zia M, Chung B, Sober SJ, and Bakir MS, "Fabrication and characterization of 3D multi-electrode array on flexible substrate for *in vivo* EMG recording from expiratory muscle of songbird," in IEDM Tech. Dig, 12 2018, pp. 29.4.1–29.4.4.

[33]. Neto JP et al., "Does impedance matters when recording spikes with polytrodes," Frontiers Neurosci, vol. 12, p. 715, 10 2018.

[34]. Chung T, Wang JQ, Wang J, Cao B, Li Y, and Pang SW, "Electrode modifications to lower electrode impedance and improve neural signal recording sensitivity," J. Neural Eng, vol. 12, no. 5, 2015, Art. no. 56018.

[35]. Ludwig KA, Langhals NB, Joseph MD, Richardson-Burns SM, Hendricks JL, and Kipke DR, "Poly (3,4-ethylenedioxythiophene) (PEDOT) polymer coatings facilitate smaller neural recording electrodes," J. Neural Eng, vol. 8, no. 1, 2011, Art. no. 14001.
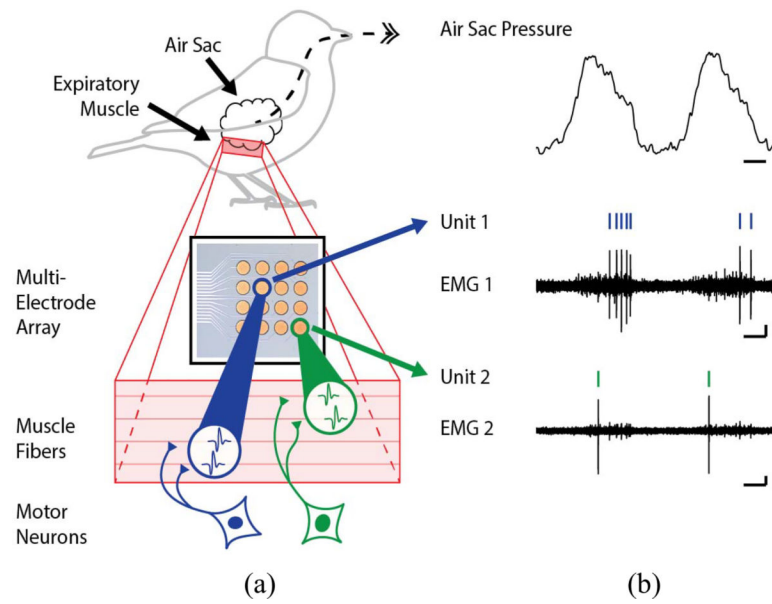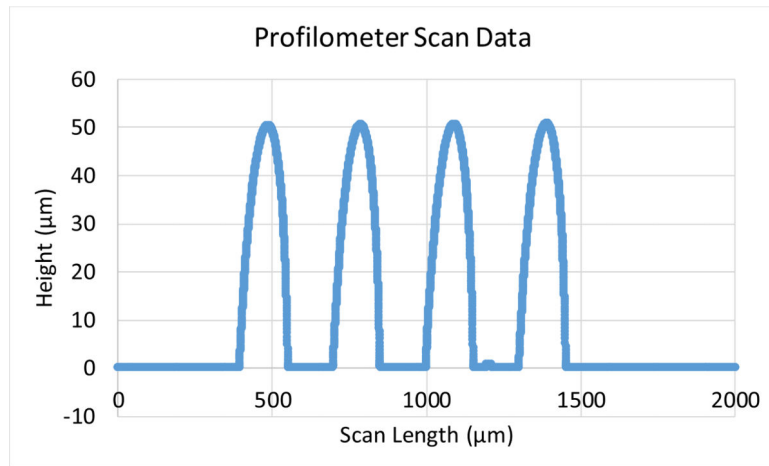
Fig. 1.
Experimental setup for measuring the EMG activity. (a) Multi-electrode arrays are used to measure the EMG activity of the expiratory muscles. (b) Air pressure and spike data-tick marks indicate spike times.
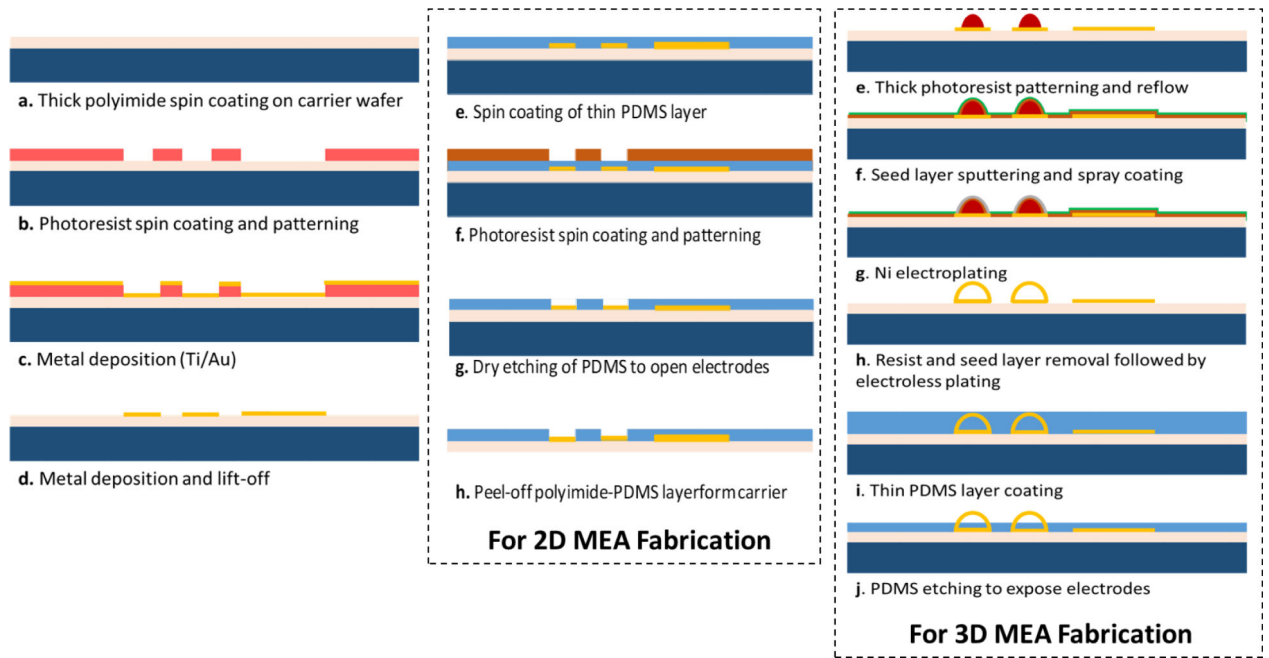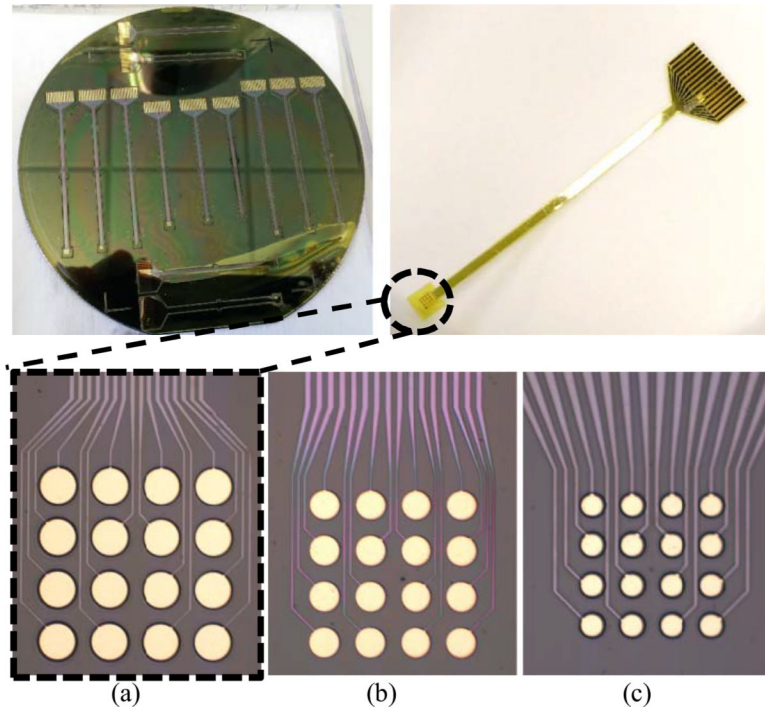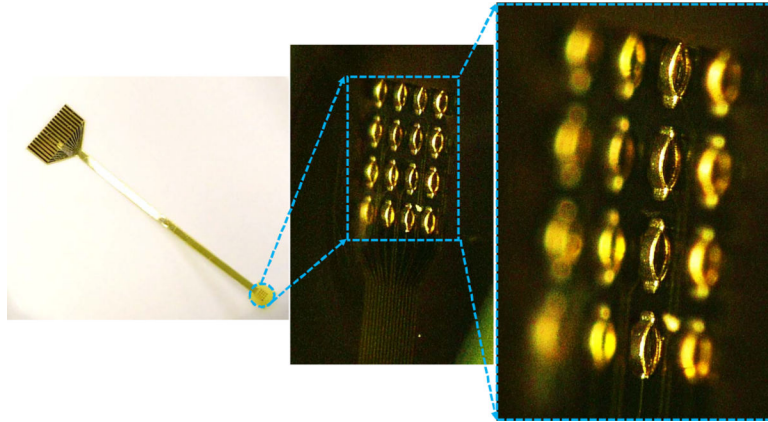
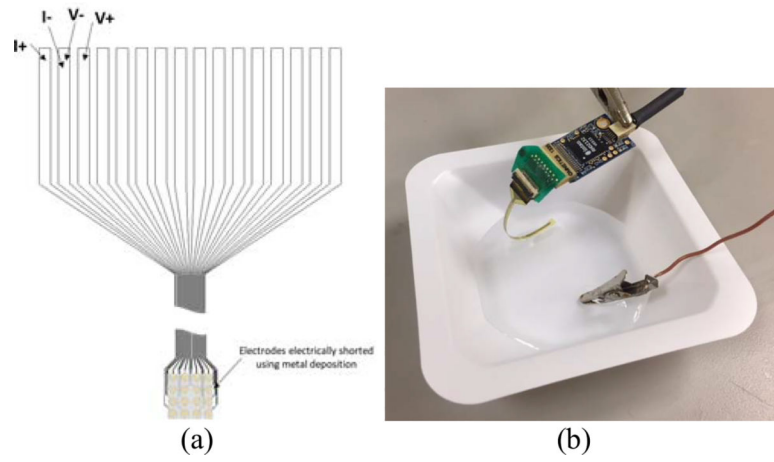**Fig. 2.**
Fabrication process flow for 2-D and 3-D MEAs.

Fig. 3.
Profilometer scan showing the hemispherical structures formed using the reflow process.

Fig. 4.
Optical image showing the fabricated electrodes. (a) 200-μm diameter, 300-μm pitch. (b) 125-μm diameter, 200-μm pitch. (c) 50-μm diameter, 100-μm pitch.
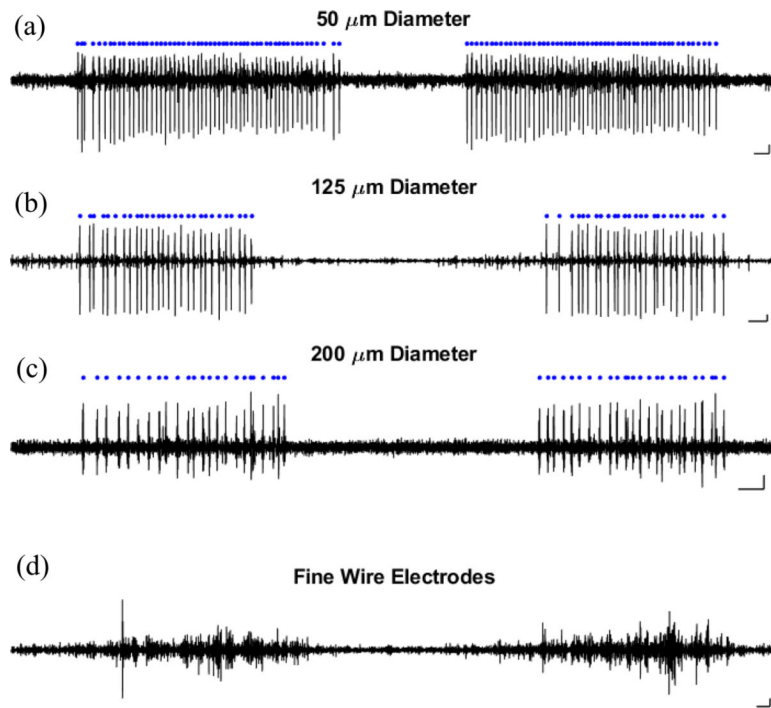
Fig. 5.
3-D optical images of the fabricated 3-D MEAs.

(a)   (b)

Fig. 6.
(a) Schematic of four-point dc resistance measurement across traces for each electrode array.
(b) Image of impedance measurement at 1000 Hz, where each electrode array is submerged in a grounded bath of saline.
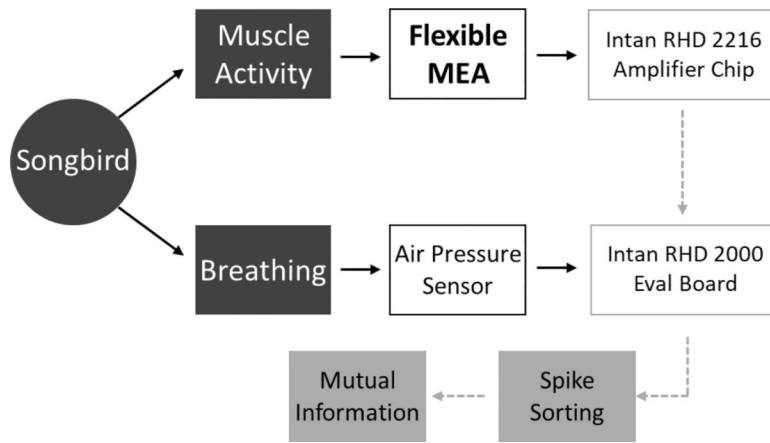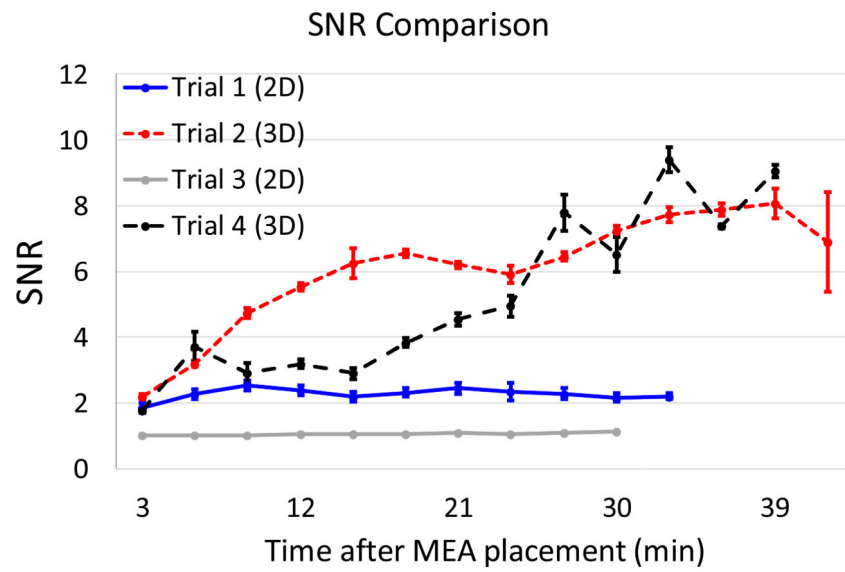
Fig. 7.
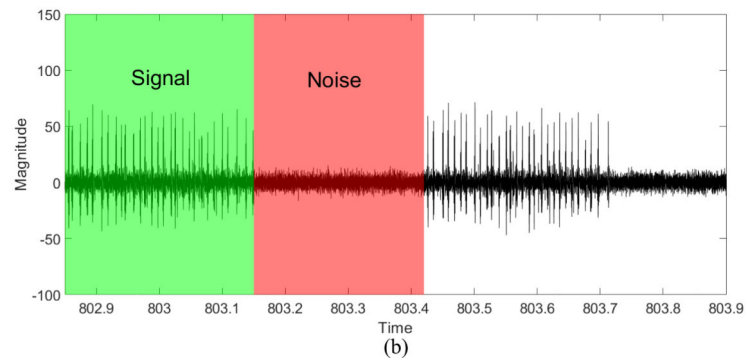Data collection flowchart [32].

Fig. 8.
EMG recordings of expiratory muscle activity using two types of devices. EMG recorded using (a)–(c) MEAs and (d) a pair of fine-wire electrodes.

SNR Comparison

(a)

(b)

Fig. 9.
(a) SNR comparison for the fabricated 2-D and 3-D MEAs. (b) Signal and noise regions of the measured EMG.